Cellulose/Polypropylene Composites: Influence of the Molecular Weight and Concentration of Oxidatively Degraded and Maleated Polypropylene Compatibilizers on Tensile Behavior

Kensuke Miyazaki,[1] Kyosuke Moriya,[1] Noriyasu Okazaki,[1] Minoru Terano,[2] Hisayuki Nakatani[1]

[1]Department of Applied and Environmental Chemistry, Kitami Institute of Technology, 165 Koen-cho, Kitami, Hokkaido 090-8507, Japan
[2]School of Materials Science, Japan Advanced Institute of Science and Technology, 1-1 Asahidai, Nomi, Ishikawa 923-1292, Japan

ABSTRACT: To improve interactions between fibrous cellulose (FC) and polypropylene (PP), oxidatively degraded polypropylene (DgPP) and maleated polypropylene (MAPP) were studied as compatibilizers. Both compatibilizers had the same mechanism, using esterification between the OH group in FC and the reactive (γ-lactone, acid, and maleic anhydride) groups in the compatibilizers. However, the adhesion style with the ester bond was considerably different because of the arrangements of the reactive groups. DgPP had reactive groups at the polymer chain end, and the tensile behavior of the FC/PP/DgPP composite exhibited comparatively ductile behavior. How-ever, MAPP had inner reactive groups, and the tensile behavior of the FC/PP/MAPP composite was quite brittle. Observation of these fracture surfaces suggested that the adhesion performance of the interface between FC and PP was strongly influenced by the arrangements of the reactive group. In addition, the performance was influenced by the molecular weight of DgPP and by the content of maleic anhydride groups in MAPP. © 2008 Wiley Periodicals, Inc. J Appl Polym Sci 111: 1835–1841, 2009

Key words: composites; electron microscopy; fibers; mechanical properties; polyolefins

INTRODUCTION

Cellulose is one of the most abundant natural resources and has been used for the manufacture of paper for a long time. Cellulose is low-cost, high-modulus, renewable, and biodegradable. Recently, cellulose has attracted much attention as a composite material[1–10] because it has great potential for the preparation of composite materials with high modulus and renewability.

As the most popular composite based on cellulose, the composite with polypropylene (PP) has been extensively prepared. This is due to the commercial importance of PP as a material applicable to household appliances, medical wares, and automotive and other industrial products. In the case of the composite, fibrous cellulose (FC) has been generally used as the cellulose source because it has been expected instead of glass or carbon fibers. FC, however, is hydrophilic and tends to aggregate; this causes poor processability and phase separation with hydrophobic PP.

The preparation of the applicable composite has been studied in the modification of FC surfaces with maleated polypropylene (MAPP),[1,6,8,9,11,12] a surfactant,[12] isocyanate coupling,[13,14] and corona discharge.[15,16] In our previous work, as a novel compatibilizer, we reported that oxidatively degraded polypropylene (DgPP) is very useful.[17] These compatibilizers play an important role in converting the hydrophilic FC surface to a hydrophobic one. The mechanism is a similar binding reaction between the OH group on the FC surface and the reactive groups in the compatibilizers. These compatibilizers adhere to the FC surface by the reaction. The adhesion style, however, is considerably different because of the arrangements of the reactive groups in the compatibilizers. One style involves adherence at the compatibilizer chain end, and the other one occurs at the inner compatibilizer chain. This difference undoubtedly affects the mechanical properties of the added composite because the distribution of applied stress is dependent on the adhesion location. In the case of polymer-type compatibilizers such as MAPP and DgPP, the compatibilizer chain adhering to FC interacts with the matrix consisting of PP chains through the entanglement of the mutual chains and brings about stronger interfacial adhesion between the PP

matrix and FC.[9] The adhesion style must be of particular importance to polymer-type compatibilizers. However, little has been investigated about this. In addition, DgPP can be easily obtained from an oxidative degradation reaction of PP at an elevated temperature and in sunlight and could be an application for recycled PP. A comparison of the compatibilizer ability of DgPP and MAPP would provide useful information for the application of DgPP.

In this study, DgPP and MAPP compatibilizers have been used as models of polymer-type compatibilizers. These compatibilizers have similar ester bonds, which are produced between the OH group in FC and the reactive groups (γ-lactone, acid, and maleic anhydride) in their polymer chains. The adhesion styles using the ester bond, however, are considerably different, so DgPP has the reactive group at the chain end[18] and MAPP has one in the inner chain.[9,19] These additive effects on the tensile behavior of FC/PP composites have been extensively studied, including the dependence of the molecular weight of DgPP and the reactive group content in MAPP.

EXPERIMENTAL

Materials

PP (meso pentad fraction = 98%) was supplied by Japan Polypropylene Co. (Yokkaichi, Japan). The number-average molecular weight (M_n) and polydispersity [weight-average molecular weight/number-average molecular weight (M_w/M_n)] of PP were 4.6×10^4 and 5.7, respectively. PP was reprecipitated from a boiling xylene solution into methanol and dried at 60°C for 8 h, and it was used as samples without an antioxidant.

FC (W-100GK) was donated by Nippon Paper Chemicals Co., Ltd. It was dried in a desiccator for 7 days before preparation.

Two kinds of MAPP were purchased from Sigma–Aldrich (St. Louis, MO). The MAPPs with lower (ca. 0.6 wt %) and higher (ca. 8 wt %) maleic anhydride contents were denoted LMAPP and HMAPP, respectively. The melt index of LMAPP was 115 g/10 min (190°C/2.16 kg). The M_n and M_w/M_n values of HMAPP were 3.9×10^3 and 2.3, respectively.

Preparation of DgPP

PP was molded into a thin film (50 µm) by compression molding at 190°C under 50 MPa for 5 min. It was put into a vial and was allowed to stand in the heating block in air. Thermal oxidative degradation was carried out at 130°C for 10 or 18 h. The PPs obtained after 10 and 18 h were called LDgPP (M_n = 1.0×10^4, M_w/M_n = 2.0) and HDgPP (M_n = $5.0 \times$

10^3, M_w/M_n = 2.3), respectively. The total contents of the oxidation compounds (γ-lactone and acid compounds) were calculated from the peak area between 2.1 and 2.3 ppm in the ^{1}H-NMR spectra.[17] In the case of LDgPP, the total content calculated from the area was about 0.9 mol %, whereas that of HDgPP was about 1.6 mol %.

Preparation of the composites

Composites were prepared with an Imoto Seisaku-syo IMC-1884 melting mixer (Kyoto, Japan). After a small amount (ca. 0.5 wt %) of a phenolic antioxidant (AO-60, Adekastab) was added, mixing was performed at 180°C and 60 rpm for 5 min. The obtained composites were molded into films (100 µm) by compression molding at 190°C under 5 MPa for 5 min.

Gel permeation chromatography analysis

A sample in a small vial was dissolved in 5 mL of o-dichlorobenzene with 2,6-di-t-butyl-p-cresol added as an antioxidant, and the obtained sample solution was directly measured by gel permeation chromatography. The molecular weight was determined by gel permeation chromatography (SSC-7100, Senshu, Tokyo, Japan) with styrene–divinylbenzene gel columns (HT-806M, Shodex) at 140°C with o-dichlorobenzene as a solvent.

Nuclear magnetic resonance spectroscopy and Fourier transform infrared spectrometer measurements

The ^{1}H-NMR spectrum of degraded PP was measured with a Varian Gemini-300 spectrometer (Palo Alto, CA) at 120°C on a 10% (w/v) solution in hexachloro-1,3-butadiene. 1,1,2,2-Tetrachloroethane-d_2 was added as an internal lock and used as an internal chemical shift reference.

The Fourier transform infrared spectrum was measured with a PerkinElmer Spectrum One spectrometer (Waltham, MA) with a film sample.

Tensile testing

The stress–strain behavior was observed with a Shimadzu EZ-S (Kyoto, Japan) at a crosshead speed of 5 mm/min. The sample specimens were cut into dimensions of $30 \times 2 \times 0.1$ mm^3, and the gauge length was 10 mm. All tensile testing was performed at 18°C. The values of Young's modulus were obtained from the slope of the stress–strain curve (until ca. 1% of the strain value). All obtained results were the average values of 10 measurements.
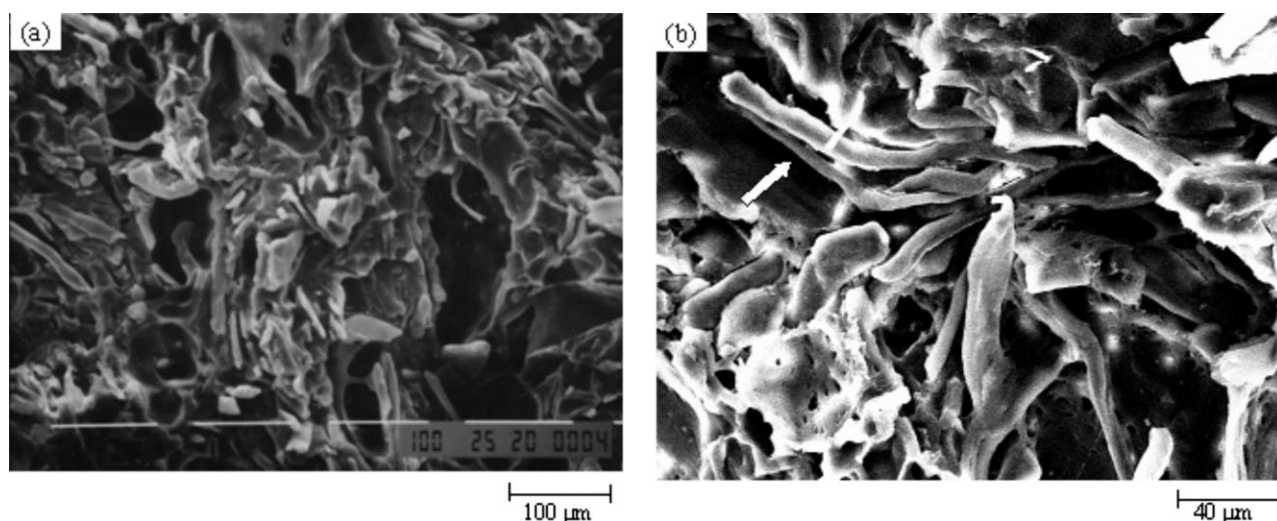
Figure 1 SEM micrographs of fracture surfaces of an FC (30 wt %)/PP (70 wt %) composite: (a) low magnification and (b) high magnification. The arrow indicates aggregated FCs.

Scanning electron microscopy (SEM) measurement

The morphology of the composite was examined with a JEOL JSM-T200 (Tokyo, Japan) at 25 kV. The plate of the composite was fractured in liquid nitrogen, and then the fractured surface was sputter-coated with gold.

Differential scanning calorimetry (DSC) measurements

DSC measurements were made with a Mettler DSC 820 (Küsnacht, Switzerland). Samples of about 5 mg were sealed in aluminum pans. The measurement of the samples was carried out at a heating rate of 20°C/min under a nitrogen atmosphere.

Wide-angle X-ray diffraction measurement

Wide-angle X-ray diffraction diffractograms were recorded in reflection geometry at 2° (2θ/min) under Ni-filtered Cu Kα radiation with a Rigaku Rint 1200 diffractometer (Tokyo, Japan).

RESULTS AND DISCUSSION

SEM micrographs of fractured surfaces of the FC/PP composites are shown in Figure 1. In Figure 1(a), the micrograph of the FC (30 wt %)/PP (70 wt %) composite clearly shows that there are many ellipse-like holes in the PP matrix. As shown in Figure 1(b), the holes are the imprints of aggregated FCs. In addition, the edges of the holes are quite smooth, and the FCs are not fractured. These results suggest that the interfacial adhesion between FC and PP is poor and requires improvement.

As shown in Figure 2, a peak appears at 1745 cm^{-1} for the FC/PP composite with DgPP as well as

MAPP added. This peak does not appear for PP (see Fig. 2) and is assigned to the ester group;[8,17] this suggests that esterification occurs between OH groups in FC and reactive (γ-lactone and acid) groups in DgPP as well as maleic anhydride groups in MAPP. These grafted FCs will certainly bring about an improvement in the interface.

Figure 3 shows the stress–strain curves of FC (30 wt %)/PP (70 wt %), FC (30 wt %)/PP (69.5 wt %)/ HDgPP (0.5 wt %), and FC (30 wt %)/PP (69.5 wt %)/HMAPP (0.5 wt %) composites. The additive effects on the tensile behavior of the FC/PP composite are obviously different between the HDgPP and
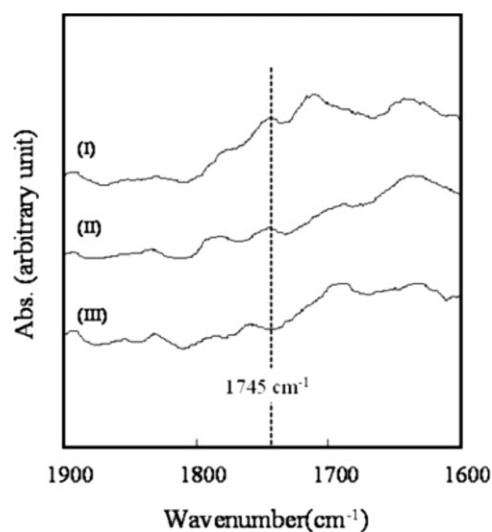
Figure 2 Fourier transform infrared spectra of PP and its composites: (I) FC (7 wt %)/PP (91 wt %)/HDgPP (2 wt %) (the content of the reactive groups was ca. 0.0003 wt %), (II) FC (7 wt %)/PP (83 wt %)/LMAPP (10 wt %) (the content of the reactive group was ca. 0.0006 wt %), and (III) PP (100%).
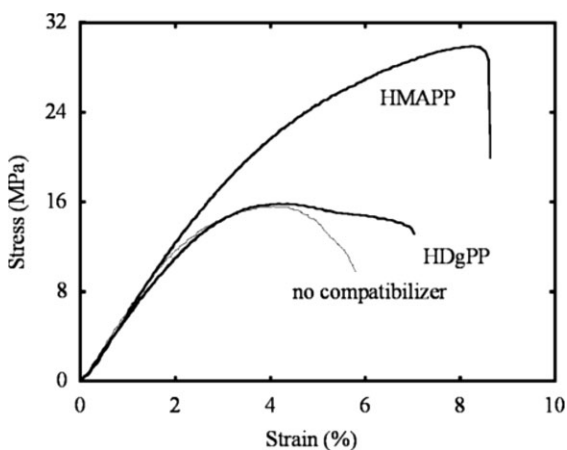
Figure 3 Stress–strain curves of an FC (30 wt %)/PP (70 wt %) composite and FC (30 wt %)/PP (69.5 wt %) composites with the addition of compatibilizers (0.5 wt %).

HMAPP compatibilizers. The curve of the composite with HDgPP added exhibits a tensile strength almost equal to that of the FC/PP composite and a broader yield region under constant stress. In contrast, although the composite with HMAPP added exhibits higher tensile strength than that of the FC/PP composite, the mechanical behavior is quite brittle (without a defined yield region). The difference in the tensile behavior is based on the chemical structures in the compatibilizer polymers. In the case of DgPP, the γ-lactone and acid groups have a greater tendency to be produced at the PP chain end.[18] In the case of MAPP, there mainly exist maleic anhydride groups in the inner PP chain.[9,19] The style of adhesion is considerably different because of the arrangements of the reactive groups, as shown in Figure 4. In the case of adhesion at the chain end, such as DgPP, stress is intensively applied in one direction along the attached polymer chain, and the chain is unidirectionally stretched from FC (see Fig. 4). If there are few chain entanglements between the chain and the PP matrix chain, FC is easily pulled out from the PP matrix without bending and fracturing. The broader yield region under constant stress likely originates from the pulling-out process because the stress should be constant during the process. However, MAPP has adhesion points in the inner chain. The adhesion location implies that the applied stress is distributed within one chain, as illustrated in Figure 4. This means that the MAPP chain is bidirectionally stretched from FC, and the dissolution of entanglements becomes hard. In this case, it seems that FC is tightly linked to the PP matrix, and the fracture of the composite accompanies FC deformations such as bending and fracturing. The brittle behavior of the composite is likely due to these FC-destructive deformations, by which the formation of a void in the PP matrix is simultaneously caused.

These explanations can be substantiated by consideration of the SEM micrographs in Figure 5, which shows the fractured surfaces of the FC/PP composite with the HDgPP and HMAPP compatibilizers added. Figure 5(a) reveals that FC coated with a polymer layer is pulled out from the PP matrix (see the arrows). This FC is unbending and unfracturing. This indicates that the linkage between HDgPP and the PP chains is very weak. In contrast, as shown in Figure 5(b), the fracturing of FC can be observed in the composite with HMAPP added (see arrow). This means that the stress is directly applied to FC without pullout. These results support the idea that the stress–strain curves exactly reflect the kind of adhesion style.

The molecular weight of LDgPP is 2 times higher than that of HDgPP (see the Experimental section). The addition of LDgPP implies that the entanglement point between the PP chain increases, and the adhesion strength of the interface between the FC and PP matrix becomes stronger. As expected, the maximum stress (21 ± 0.2 MPa, the average of 10 measurements) of the FC/PP/LDgPP composite is about 30% higher than that (16 ± 0.9 MPa, the average of 10 measurements) of the FC/PP/HDgPP composite (see Fig. 6), demonstrating that the interface adhesion strength becomes stronger because of the increase in the entanglement point. It can be observed here that the yield region is considerably smaller than that of the composite with HDgPP added. This behavior implies that interface exfoliation occurs when FC is being pulled out from the PP matrix. Figure 7 shows an SEM micrograph of the fractured surfaces of an FC/PP composite with the
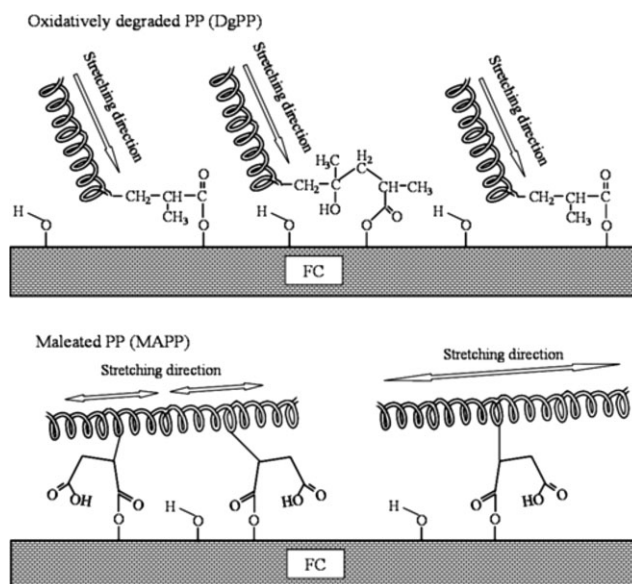
**Figure 4** Model of DgPP and MAPP chains bound to an FC particle in composites.
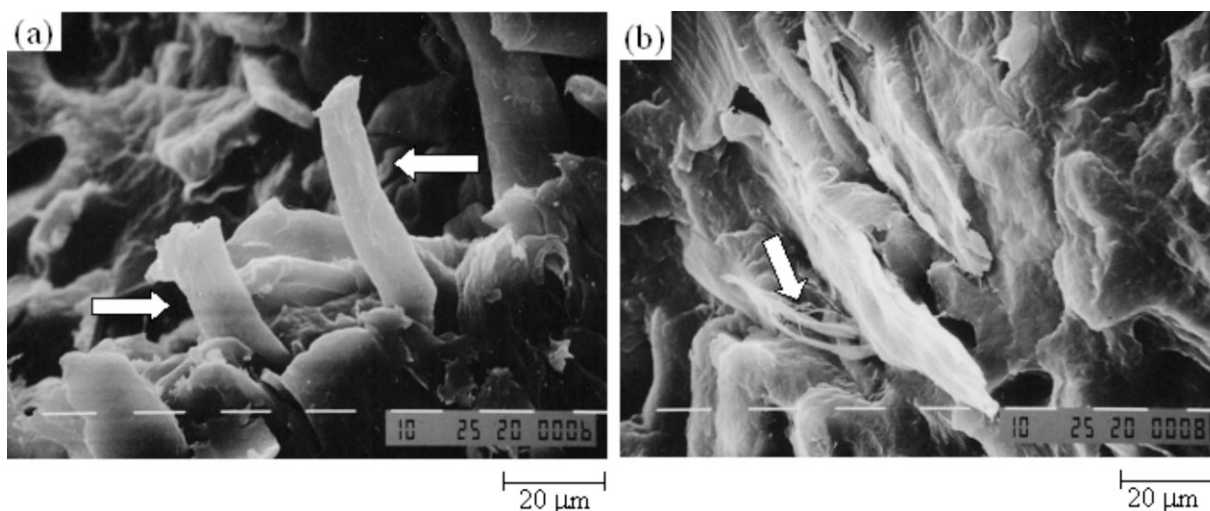
Figure 5 SEM micrographs of fracture surfaces of composites: (a) FC (30 wt %)/PP (67.5 wt %)/HDgPP (2.5 wt %) and (b) FC (30 wt %)/PP (69 wt %)/HMAPP (1 wt %). The contents of the reactive groups were similar (0.0004 and 0.0008 wt %, respectively). The arrows indicate pulled and fractured FCs, respectively.

addition of LDgPP with the same reactive group content (ca. 0.0004 wt %) as that of HDgPP. The pullout of FC is incomplete, and the fractured surface is partially turned up. The applied stress is likely over the maximum elastic modulus of FC. This indicates an increase in the interface adhesion strength. In addition, the adhesion strength seems not to be as strong as that of the composite with HMAPP added because fracturing of FC is not seen.
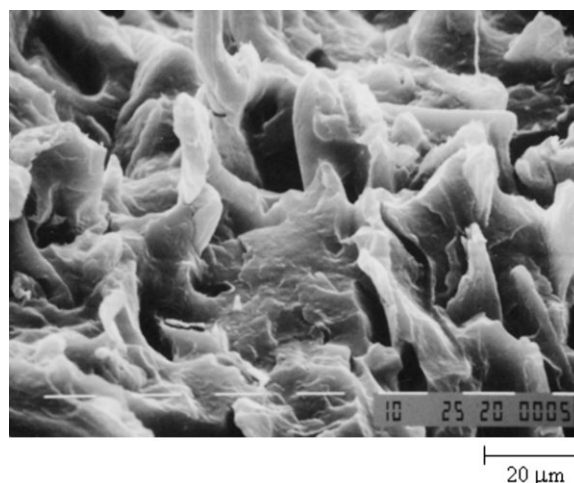
The stress–strain curves of composites with LMAPP added are shown in Figure 8. The tensile strength of the composite with LMAPP added is considerably lower because of its extremely lower content of maleic anhydride groups (ca. a tenth of that of HMAPP). This behavior suggests that a certain content of maleic anhydride groups is directly linked to the tensile strength of the composite. In fact, as shown in Figure 9, the fracturing of FC can be observed in the composite with the same maleic anhydride group content and in the composite with HMAPP added.

Interestingly, the composite with LMAPP added has a considerably higher Young's modulus than the other composites (see Fig. 8 and Table I). This suggests that the interface adhesion strength is independent of the value of Young's modulus. To clarify the additive effect of LMAPP on the PP matrix, a PP (90 wt %)/LMAPP (10 wt %) polymer blend, with the amount of LMAPP increased, was prepared, and its thermal properties were investigated with DSC
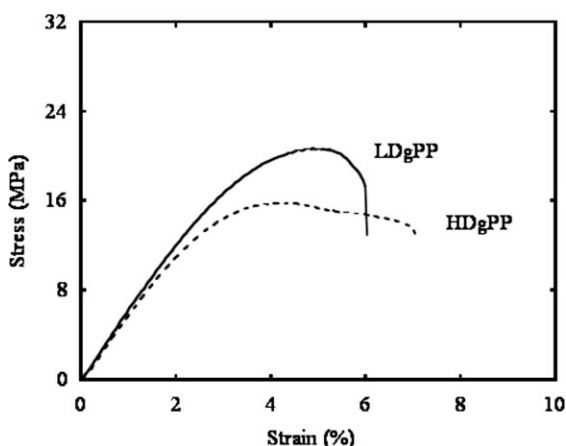
Figure 6 Stress–strain curves of FC (30 wt %)/PP (69.5 wt %)/DgPP (0.5 wt %) composites.
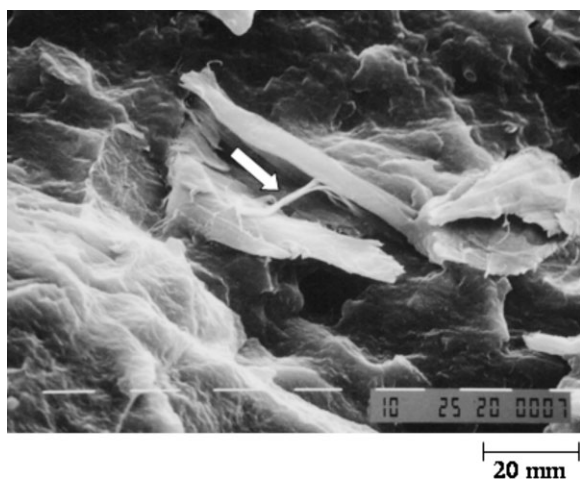

Figure 7 SEM micrograph of fracture surfaces of an FC (30 wt %)/PP (66 wt %)/LDgPP (4 wt %) composite. The content of the reactive groups was about 0.0004 wt %.
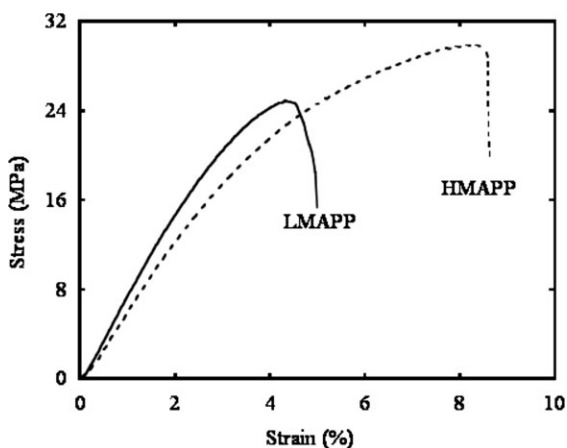
Figure 8 Stress–strain curves of FC (30 wt %)/PP (69.5 wt %)/MAPP (0.5 wt %) composites.

measurements. Figure 10 shows the DSC curve of PP (90 wt %)/LMAPP (10 wt %). Only one melting point can be observed, and another melting point, such as the melting point corresponding to the maleic anhydride side chain group, is unseen. In the case of the FC (30 wt %)/PP (67 wt %)/LMAPP (3 wt %) composite, however, another new melting point appears in a higher temperature region (see Fig. 11). This implies that the existence of FC affects PP/LMAPP. As shown in Figure 12, however, the crystal form of PP in the FC/PP/LMAPP composite is the α form (monoclinic), the same as that of common PP, and it exhibits no change in the crystalline morphology. The higher new melting point originates not from another crystal structure but from a thicker lamella with the same crystal structure. FC likely acts as a nucleating agent, leading to an increase in the crystallization rate of the PP/LMAPP

Figure 9 SEM micrograph of fracture surfaces of an FC (30 wt %)/PP (56 wt %)/LMAPP (14 wt %) composite. The content of the reactive groups was about 0.0008 mol %.

TABLE I
Young's Modulus of FC (30 wt %)/PP (69.5 wt %) Composites Containing Compatibilizers (0.5 wt %)

Compatibilizer	HDgPP	LDgPP	HMAPP	LMAPP
Young's modulus (MPa)	592 ± 36	634 ± 49	636 ± 54	782 ± 15

part, although the nucleating mechanism is unclear. The higher melting point would be due to the nucleation effect. The produced lamella turns out to be considerably thick from the higher melting point around 170°C. The higher Young's modulus of the FC/PP/LMAPP composite is derived from such thick lamellae. FC seems to have no ability of nucleation against the PP/HMAPP composite. HMAPP is believed to cover the entire surface of FC because of the higher maleic anhydride content. Therefore, the nucleation effect seems to not occur in the FC/PP/HMAPP composite.

CONCLUSIONS

With the aim of enhancing compatibility between FC and PP, DgPP and MAPP compatibilizers were studied. Both compatibilizers had the same improvement mechanism using esterification between the OH group in FC and the reactive (γ-lactone, acid, and maleic anhydride) groups in the polymer chains. However, the adhesion style using the ester bond was considerably different because of the arrangements of the reactive groups. The DgPP compatibilizer had the reactive groups at the polymer chain end. In the case of the adhesion of the chain at this position, stress was intensively applied in one direction along the chain, and the chain unidirectionally stretched from FC. The MAPP compatibilizer had adhesion points in the inner chain, so the applied stress was distributed within one chain.
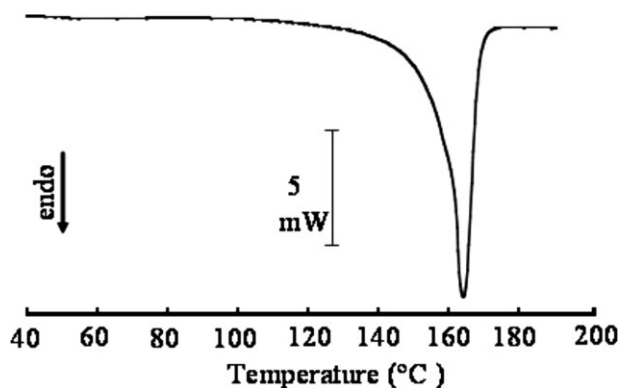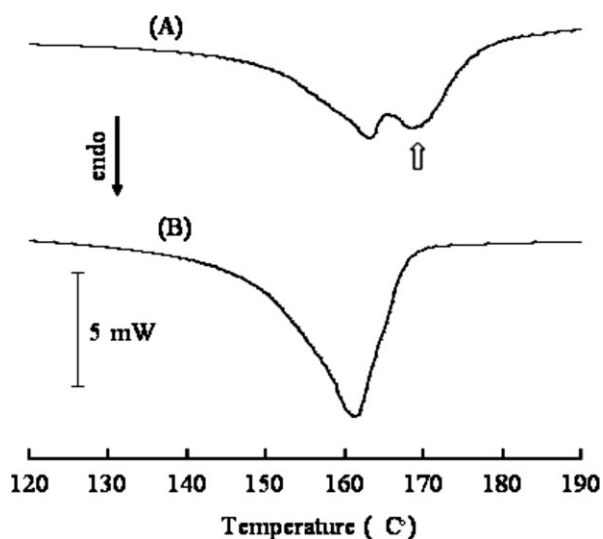

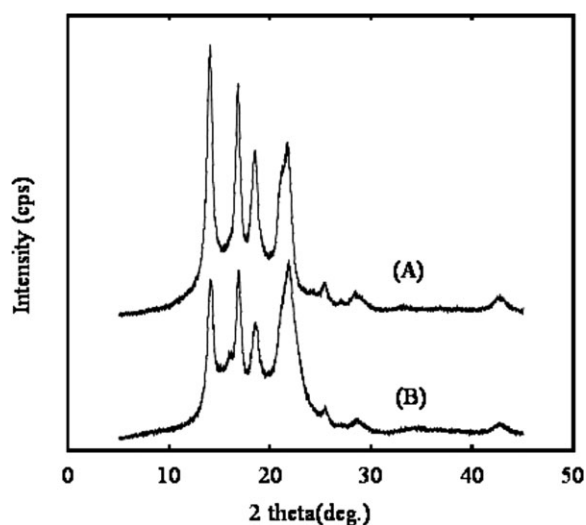**Figure 10** DSC curve of a PP (90 wt %)/LMAPP (10 wt %) polymer blend.

The stress–strain curve of the FC/PP/HDgPP composite exhibited lower tensile strength and a broader yield region, and this indicated that the composite was typically a ductile material. In contrast, although the FC/PP/HMAPP composite had higher tensile strength, the tensile behavior was quite brittle. In the SEM micrograph of the fractured surface of the FC/PP/HDgPP composite, FC was shown to be pulled out from the PP matrix without bending or fracturing. This supported the idea that the broader yield region observed originated from the FC pullout process. However, in the micrograph of the FC/PP/HMAPP composite, the fracturing of FC was observed, indicating that the stress was directly applied to FC without pullout. This suggested that the characteristics of the tensile behavior, such as the higher tensile strength and brittleness, were based on the mechanism in which the applied stress was directly transmitted to FC. These results implied that arrangements of the reactive groups in the compatibilizers directly affected the tensile behavior of the FC/PP composite.

In the DgPP compatibilizer, the adhesion strength of the interface between the FC and PP matrix was found to become considerably stronger with an increase in the molecular weight of the compatibilizer. However, in the MAPP compatibilizer, a certain content of maleic anhydride groups was found to be directly linked to the tensile strength of the composite by a comparison of HMAPP with LMAPP having a considerably lower content of maleic anhydride groups. In addition, in the case of the FC/PP/

Figure 12 Wide-angle X-ray diffraction profiles: (A) PP and (B) FC (30 wt %)/PP (67 wt %)/LMAPP (3 wt %).

LMAPP composite, a thicker lamella was produced and was found to give a higher Young's modulus to the composite.

References

1. Takase, S.; Shiraishi, N. J Appl Polym Sci 1989, 37, 645.
2. Maldas, D.; Kokta, B. V.; Daneault, C. J Appl Polym Sci 1989, 37, 751.
3. Raj, R. G.; Kokta, B. V.; Maldas, D.; Daneault, C. J Appl Polym Sci 1989, 37, 1089.
4. Hedenberg, P.; Gatenholm, P. J Appl Polym Sci 1996, 60, 2377.
5. Zhang, F.; Qiu, W.; Yang, L.; Endo, T. J Mater Chem 2002, 12, 24.
6. Qiu, W.; Zhang, F.; Endo, T.; Hirotsu, T. J Appl Polym Sci 2003, 87, 337.
7. Qiu, W.; Zhang, F.; Endo, T.; Hirotsu, T. J Appl Polym Sci 2004, 91, 1703.
8. Felix, J. M.; Gatenholm, P. J Appl Polym Sci 1991, 42, 609.
9. Qiu, W.; Zhang, F.; Endo, T.; Hirotsu, T. J Appl Polym Sci 2004, 94, 1326.
10. Hristov, V. N.; Vasileva, S. T.; Krumova, M.; Lach, R.; Michler, G. H. Polym Compos 2004, 25, 521.
11. Ljungberg, N.; Bonini, C.; Bortolussi, F.; Boisson, C.; Heux, L.; Cavaillé, J. Y. Biomacromolecules 2005, 6, 2732.
12. Baiardo, M.; Frisoni, G.; Scandola, M.; Licciardello, A. J Appl Polym Sci 2002, 83, 38.
13. Joy, C.; Gauthier, R.; Escoubes, M. J Appl Polym Sci 1996, 61, 57.
14. Botaro, V. R.; Gandini, A. Cellulose 1998, 5, 65.
15. Belgacem, M. N.; Bataille, P.; Sapieha, S. J Appl Polym Sci 1994, 53, 1447.
16. Massines, F.; Gouda, G. J Phys D 1998. 31, 3411.
17. Miyazaki, K.; Okazaki, N.; Terano, M.; Nakatani, H. J Polym Environ, to appear.
18. Adams, J. H. J Polym Sci Part A-1: Polym Chem 1970, 8, 1077.
19. Heinen, W.; Rosenmöller, C. H.; Wnzel, C. B.; de Groot, H. J. M.; Lugtenburg, J. Macromolecules 1996, 29, 1151.

Figure 11 DSC curves of composites: (A) FC (30 wt %)/PP (67 wt %)/LMAPP (3 wt %) and (B) FC (30 wt %)/PP (67 wt %)/HMAPP (3 wt %).